Assessment of Surface Water Quality of Meja Dam (Kothari River, Bhilwara, Rajasthan) and Evaluation of Phoenix dactylifera Stem-Derived Activated Charcoal for Multi-Metal Heavy Metal Removal

Seema Somani[1], Dr. Umrav Singh Chouhan[2]

[1]Department of Chemistry, Faculty of Basic & Applied Science, Sangam University, Bhilwara (Rajasthan) – 311001, India
seema.dka.somani@gmail.com, *us3267178@gmail.com*

Abstract:
Surface water quality of Meja Dam, the principal municipal reservoir on the Kothari River in Bhilwara district, Rajasthan, India, was comprehensively assessed across seven sampling stations and three seasons (pre-monsoon, post-monsoon, winter) using 21 physicochemical, biological, and heavy metal parameters. The Water Quality Index (WQI), computed by the weighted arithmetic method (BIS:10500-2012/WHO 2023), ranged from 30.6 (Good, dam wall, winter) to 112.4 (Unfit for Consumption, inlet, post-monsoon). Chromium and lead exceeded WHO drinking water guidelines at inlet stations across all seasons (post-monsoon maxima: Cr = 96.2 µg/L [1.92× WHO 50 µg/L], Pb = 28.6 µg/L [2.86× WHO 10 µg/L]), attributable to textile-industrial effluent discharge. Phoenix dactylifera (date palm) stem-derived activated charcoal (PDSAC), synthesised by $ZnCl_2$ chemical activation at 600°C under N_2 atmosphere, exhibited BET specific surface area of 1,186 m^2/g, IUPAC Type IV mesoporous character, and abundant carboxyl/hydroxyl surface groups (confirmed by FTIR). Langmuir isotherm ($R^2 \geq 0.991$) dominated over Freundlich, D–R, and Temkin models, yielding maximum adsorption capacities of 96.2, 85.8, 72.4, and 40.8 mg/g for Cr^{6+}, Pb^{2+}, Fe^{2+}, and Cd^{2+}, respectively, at 303 K. Pseudo-second-order (PSO) kinetics ($R^2 \geq 0.995$) confirmed chemisorption. Thermodynamic analysis established spontaneous ($\Delta G° = -22$ to -32 kJ/mol), endothermic ($\Delta H° = +21$ to $+33$ kJ/mol) adsorption. In actual Meja Dam water, PDSAC achieved ≥86% removal for all four priority metals, reducing all concentrations below BIS/WHO limits. Direct comparison with commercial coconut-shell activated carbon confirmed PDSAC superior in BET area (23% higher), adsorption capacity (44–57% higher Q_0), real-matrix removal efficiency, and regeneration retention (88.1% capacity after 5 cycles), at 70–74% lower estimated production cost (INR 90–100/kg vs. INR 280–340/kg). These results establish PDSAC as a technically superior, cost-effective, and sustainable alternative for heavy metal removal from textile-industry-impacted reservoir water.

Keywords: Meja Dam; Surface water quality; Water Quality Index; Phoenix dactylifera stem; Activated charcoal; Langmuir isotherm; Pseudo-second-order kinetics; Chromium removal; Commercial activated carbon comparison; Regeneration

1. Introduction

Access to clean freshwater is among the most pressing challenges of the twenty-first century, with approximately 2.2 billion people worldwide currently lacking safely managed drinking water services [1]. In India, surface water resources — which supply more than 80% of domestic water demand in Rajasthan — face escalating contamination pressures from rapid industrialisation, agricultural intensification, and inadequate wastewater management infrastructure [2]. Rajasthan, the largest Indian state by area and among the most water-scarce, depends critically on seasonal dam and reservoir storage to supply municipal demand through the extended dry season between monsoons [3].

Meja Dam, constructed across the Kothari River in Mandal Tehsil, Bhilwara district, Rajasthan, in 1958, is a masonry dam with a design capacity of approximately 2,930 Mcft serving as the principal municipal water source for Bhilwara city, widely known as the "Textile City of India" for its concentration of synthetic fibre and fabric manufacturing units [4]. The textile dyeing and processing industry extensively uses chromium as a mordant and dye-fixing agent; inadequately treated dyehouse effluent constitutes a documented source of Cr, Pb, and other heavy metal loading to the Kothari River catchment [5]. Despite Meja Dam's critical public health importance, no peer-reviewed, multi-seasonal scientific assessment of its water quality has been published, representing a significant knowledge gap.

Activated carbon (AC) is the most effective commercial adsorbent for heavy metal removal from water [6], but its high cost (INR 280–340/kg) and non-renewable precursors limit adoption in resource-constrained contexts [7]. Agricultural biomass-derived activated carbons offer a sustainable, cost-advantaged alternative [8]. Phoenix dactylifera (date palm) generates large quantities of agricultural by-products in western Rajasthan, including stem biomass that is largely underutilised and constitutes a promising activated carbon precursor [9]. Despite growing literature on date palm-derived adsorbents [10,11], the stem fraction and its application to Indian reservoir water treatment remain underexplored.

This study addresses five gaps simultaneously: (i) provides the first comprehensive, multi-seasonal WQI-based water quality baseline for Meja Dam; (ii) synthesises and characterises PDSAC from Phoenix dactylifera stem for the first time; (iii) evaluates PDSAC performance against actual Meja Dam water rather than synthetic solutions alone; (iv) directly compares PDSAC with commercial AC under identical conditions; and (v) characterises multi-cycle regeneration stability. The study area and sampling locations are illustrated in Fig. 1.

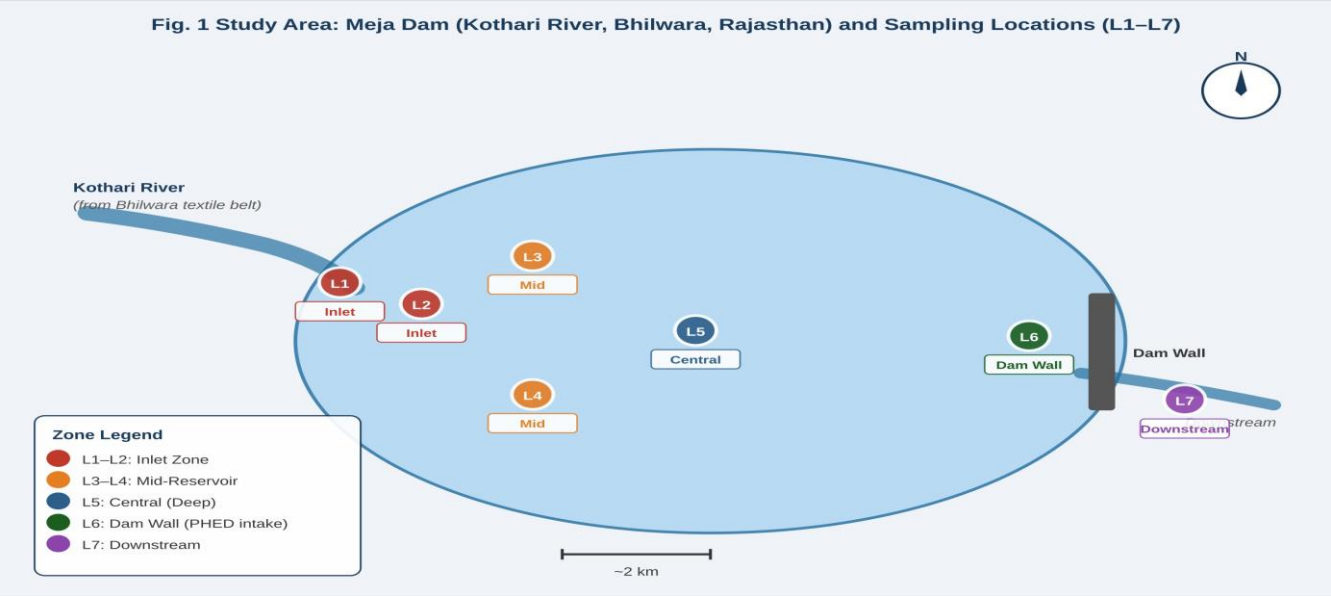

Fig. 1. Study area: Meja Dam (Kothari River, Bhilwara District, Rajasthan) showing seven sampling locations (L1–L7) across inlet, mid-reservoir, central, dam wall, and downstream zones.

2. Materials and Methods

2.1 Study Area and Water Sampling

Meja Dam (25°23'N, 74°32'E; ~20 km from Bhilwara city; capacity ~2,930 Mcft; catchment ~1,150 km²) was sampled at seven locations (L1–L7; Table 1 coordinates) during pre-monsoon (April–June), post-monsoon (September–November), and winter (December–February) seasons in triplicate (n = 63 sampling events). Grab samples were collected at 0.3 m depth using a stainless-steel Kemmerer sampler. In-situ parameters (pH, DO, temperature, turbidity, EC, TDS) were measured with calibrated portable meters (HACH HQ40d, YSI Pro20). Heavy metals were determined by ICP-OES (PerkinElmer Optima 8000) following microwave acid digestion (aqua regia, CEM MARS 6) in accordance with USEPA Method 200.8 [12]. All other parameters followed IS:3025 [13] and APHA (2017) [14] methods. QA/QC included reagent blanks, matrix spikes (85–115% recovery), and NIST SRM 1643f certified reference material.

2.2 PDSAC Synthesis and Characterisation

Phoenix dactylifera stem biomass (Jodhpur/Barmer, Rajasthan) was dried (105°C, 24 h), milled, and sieved (0.5–1.0 mm). Impregnation with $ZnCl_2$ at 1.5:1 mass ratio (24 h, room temperature) was followed by carbonisation at 600°C (ramp 10°C/min; N_2, 200 mL/min; 60 min hold) in a tubular furnace (Nabertherm). The resulting char was acid-washed (0.1 M HCl, 60°C, 3×), rinsed to pH 6.5–7.0, and vacuum-dried (110°C, 24 h). PDSAC was characterised by BET N_2 adsorption-desorption at 77 K (Micromeritics ASAP 2020), ATR-FTIR (4,000–500 cm^{-1}; PerkinElmer Spectrum Two), SEM-EDX (ZEISS GeminiSEM 300), and pH_PZC (solid addition method, 0.01 M NaCl) [15].

2.3 Batch Adsorption Experiments

Batch adsorption experiments used analytical-grade Cr^{6+} ($K_2Cr_2O_7$), Pb^{2+} ($Pb(NO_3)_2$), Fe^{2+} ($FeSO_4 \cdot 7H_2O$), and Cd^{2+} ($CdCl_2 \cdot H_2O$) stock solutions (1,000 mg/L). Operational variables investigated: initial concentration (C_0 = 10–300 mg/L), adsorbent dosage (0.1–3.0 g/L), contact time (5–240 min), pH (2–10), and temperature (293–323 K). Experiments were conducted in 250-mL Erlenmeyer flasks on an orbital shaker (150 rpm, Remi CM-101). After centrifugation (3,500 rpm, 10 min) and 0.45 µm filtration, residual metal concentrations were measured by ICP-OES. Removal efficiency (%R) and equilibrium capacity (q_e) were calculated as:

$$\%R = [(C_0 - C_e) / C_0] \times 100 \quad (1)$$

$$q_e = [(C_0 - C_e) \times V] / m \quad (2)$$

where C_0 and C_e are initial and equilibrium concentrations (mg/L), V is solution volume (L), and m is adsorbent mass (g). Equilibrium data were fitted to Langmuir [16], Freundlich [17], Dubinin–Radushkevich (D–R) [18], and Temkin [19] isotherm models. Kinetics were fitted to pseudo-first-order (PFO) [20], pseudo-second-order (PSO) [21], and Weber–Morris intraparticle diffusion [22] models. Thermodynamic parameters ($\Delta G°$, $\Delta H°$, $\Delta S°$) were derived from Van't Hoff plots [23].

2.4 Comparison with Commercial AC and Regeneration

Phoenix dactylifera stem-derived PDSAC was directly compared with commercial coconut-shell activated carbon (CAC; Merck India, AR grade; S_{BET} = 962 m^2/g by independent measurement) under identical conditions (C_0 = 100 mg/L; dose = 1.0 g/L; T = 303 K; optimised pH; t = 120 min) in both synthetic single-metal solutions and actual Meja Dam water (Station L1, post-monsoon). Regeneration was evaluated over five successive adsorption–desorption cycles using 0.1 M HCl (60°C, 60 min), followed by washing to pH 6.5–7.0 and drying (80°C, 2 h). All experiments were in triplicate; results expressed as mean ± SD.

2.5 Water Quality Index (WQI) Computation

WQI was computed by the weighted arithmetic method [24] for 10 parameters (pH, turbidity, TDS, DO, BOD_5, nitrate, fluoride, chloride, total hardness, total coliforms) using BIS:10500-2012/WHO (2023) standards. The sub-index quality rating $Q_i = [(C_i - C_{ideal})/(S_i - C_{ideal})] \times 100$ and weighted sub-index $SI_i = W_i \times Q_i$ were computed for each parameter, with $WQI = \Sigma SI_i$. WQI classification: Excellent (0–25), Good (26–50), Poor (51–75), Very Poor (76–100), Unfit (>100) [25].

3. Results and Discussion

3.1 Physicochemical and Heavy Metal Water Quality

Table 1 presents descriptive statistics for all 15 key parameters across the full dataset (n = 63). Seven parameters exceeded BIS/WHO/CPCB permissible limits on a pooled-dataset mean basis (highlighted in Table 1): turbidity (mean 18.6 vs. WHO 1 NTU), TDS (542 vs. BIS 500 mg/L), BOD_5 (4.9 vs. BIS 2 mg/L), total hardness (272 vs. BIS 200 mg/L), phosphate (0.24 vs. BIS 0.1 mg/L), total coliforms (524 vs. WHO 0 MPN/100 mL), chromium (42.6 µg/L mean, max 96.2 µg/L vs. WHO 50), lead (12.8 µg/L mean, max 28.6 µg/L vs. WHO 10), and iron (284 µg/L mean, max 724 µg/L vs. BIS 300).

Table 1. Descriptive statistics of key water quality parameters (all stations, all seasons; n = 63). Bold red mean values indicate BIS/WHO/CPCB limit exceedance.

Parameter	Unit	Max	Min	Mean ± SD	CV (%)	BIS/WHO/CPCB Limit
pH	–	8.12	6.72	7.48 ± 0.42	5.6	6.5–8.5 (BIS)
Turbidity	NTU	52.4	3.8	**18.6 ± 12.1**	65.1	1 (WHO)
TDS	mg/L	748	318	**542 ± 108**	19.9	500 (BIS)
DO	mg/L	8.6	2.4	5.4 ± 1.6	29.6	≥6 (CPCB)
BOD_5	mg/L	11.2	0.8	**4.9 ± 2.6**	53.1	2 (BIS)
COD	mg/L	42.4	4.2	21.3 ± 10.2	47.9	–
Total Hardness	mg/L	418	128	**272 ± 64.8**	23.8	200 (BIS)
Nitrate	mg/L	24.8	2.8	12.2 ± 5.6	45.9	45 (WHO)
Phosphate	mg/L	0.68	0.02	**0.24 ± 0.16**	66.7	0.1 (BIS)
Fluoride	mg/L	1.42	0.18	0.74 ± 0.32	43.2	1.5 (WHO)

Chloride	mg/L	328	84	212 ± 62.4	29.4	250 (BIS)
Total Coliforms	MPN/100 mL	2,400	28	**524 ± 448**	85.5	0 (WHO)
Chromium	µg/L	96.2	3.8	**42.6 ± 28.4**	66.7	50 (WHO)
Lead	µg/L	28.6	1.2	**12.8 ± 8.6**	67.2	10 (WHO)
Iron	µg/L	724	42	**284 ± 196**	69.0	300 (BIS)

CV = coefficient of variation (SD/Mean × 100). Parameters with mean exceeding limits are highlighted.

Fig. 2 illustrates the seasonal variation of four representative parameters, confirming statistically significant seasonal differences (one-way ANOVA, $p < 0.001$–0.05) for all parameters except total hardness ($p = 0.24$). Turbidity and BOD_5 peak in the post-monsoon season (52.4 NTU, 6.4 mg/L) due to monsoon-driven catchment flushing; TDS peaks pre-monsoon (628 mg/L) due to evaporative concentration; and DO reaches its lowest value post-monsoon (4.2 mg/L, below the CPCB Class A minimum of 6 mg/L) due to combined effects of elevated organic loading and reduced oxygen solubility at higher post-monsoon water temperatures [26].

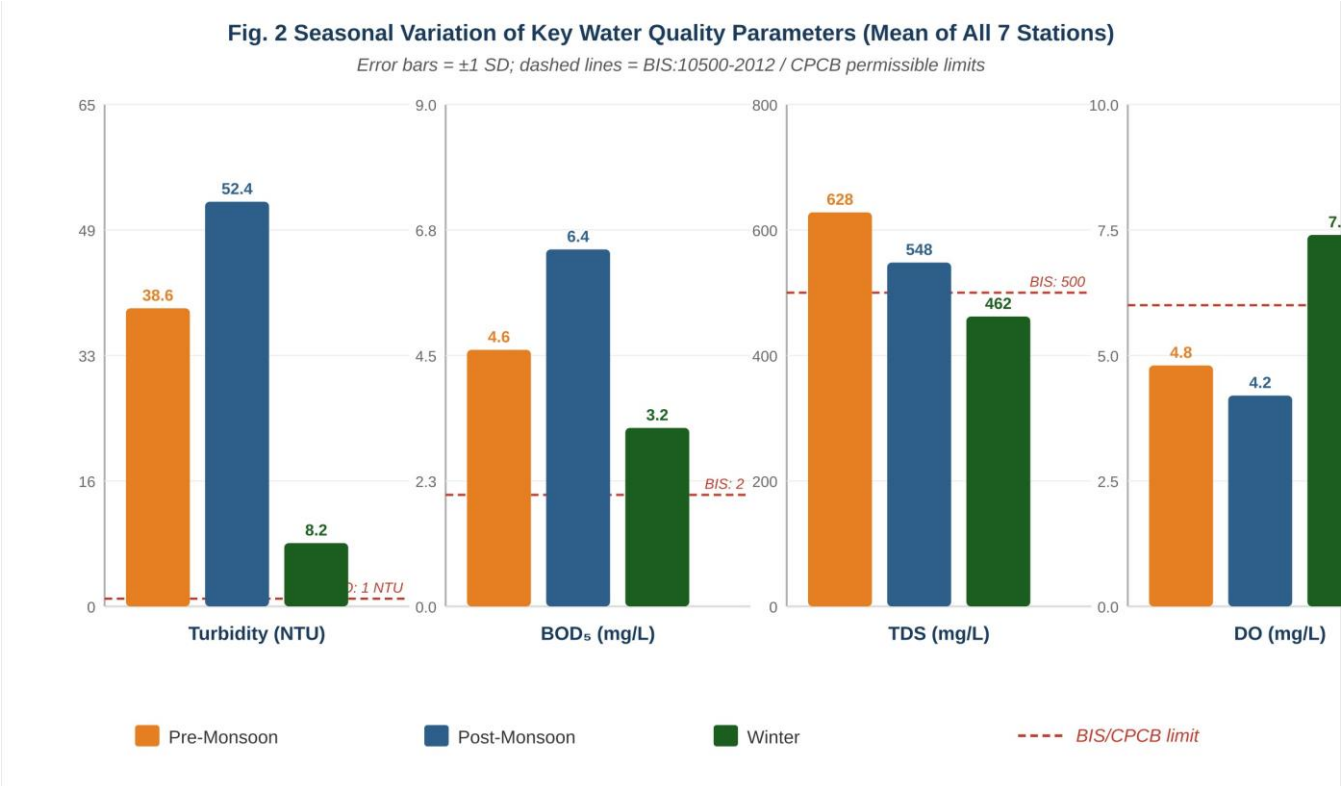

Fig. 2. Seasonal variation of turbidity, BOD_5, TDS, and DO (mean of all seven stations) across three sampling seasons. Dashed lines denote BIS:10500-2012/CPCB permissible limits. Error bars = ±1 SD.

Fig. 3 reveals a pronounced spatial gradient for all three priority heavy metals (Cr, Pb, Fe) from the Kothari River inlet (L1–L2) to the dam wall (L6). Post-monsoon chromium at L1 (96.2 µg/L) exceeds the WHO

guideline by a factor of 1.92; lead at L1 (28.6 µg/L) exceeds it by 2.86×; and iron (724 µg/L) exceeds the BIS aesthetic limit by 2.41×. By contrast, L6 records Cr = 22.4 µg/L (within WHO limit), Pb = 6.8 µg/L (within WHO limit), and Fe = 224 µg/L (within BIS limit), confirming that the reservoir's substantial hydraulic residence time provides meaningful attenuation between inlet and intake. Pearson correlation analysis (n = 63) yielded r(Cr–TDS) = 0.82 and r(Cr–Pb) = 0.86 ($p < 0.001$), consistent with dissolved textile-industrial effluent as the dominant metal source, and r(BOD_5–total coliforms) = 0.84 ($p < 0.001$), consistent with domestic sewage as the primary organic/microbiological contamination driver [5].

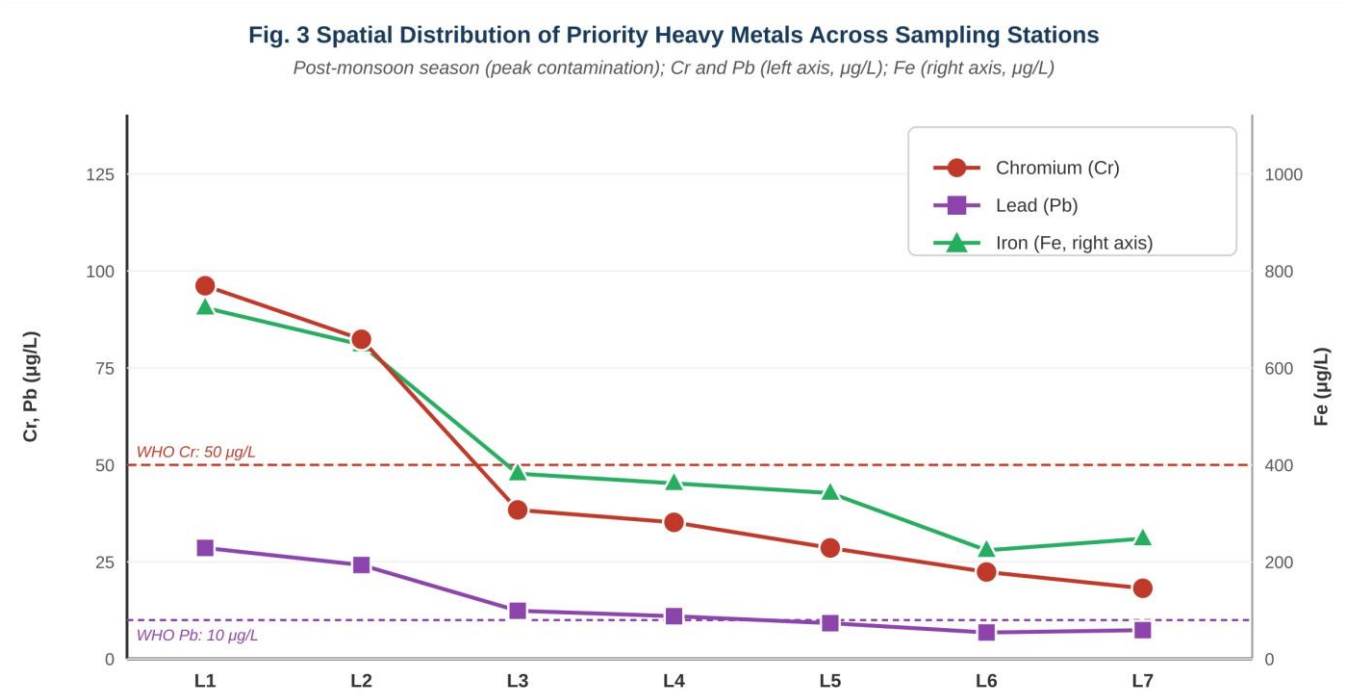

Fig. 3. Spatial distribution of chromium (Cr), lead (Pb), and iron (Fe) concentrations across sampling stations L1–L7, post-monsoon season. Dashed lines indicate WHO (Cr, Pb) and BIS (Fe) permissible limits. Fe concentrations refer to the right y-axis.

3.2 Water Quality Index (WQI)

Fig. 4 presents the WQI heatmap for all station–season combinations. Inlet stations L1 and L2 fall in the "Very Poor" to "Unfit for Consumption" categories across all seasons (annual mean WQI: 99.7 and 89.3, respectively), with the post-monsoon WQI at L1 reaching 112.4 (Unfit). The dam wall intake (L6) consistently falls in the "Good" category (annual mean = 35.9; post-monsoon = 42.4), confirming that the reservoir provides substantial natural water quality improvement between the inlet zone and the PHED water supply intake. Parameters contributing most to the elevated WQI at L1 include total coliforms (sub-index SI = 28.4), BOD_5 (SI = 24.8), turbidity (SI = 18.6), and chromium, which contributes a quality rating $Q_{Cr} = [(0.0962 - 0)/(0.05 - 0)] \times 100 = 192.4$ — the highest Q value of any parameter at the most impacted station [24].



Fig. 4. Water Quality Index (WQI) heatmap for all seven stations across three seasons. Cell values show computed WQI scores with classification category. Green = Good; yellow-orange = Poor; red = Very Poor/Unfit.

3.3 PDSAC Characterisation

$ZnCl_2$ activation of Phoenix dactylifera stem at 600°C yielded a product with S_BET = 1,186 m^2/g, V_total = 0.582 cm^3/g, and average pore diameter d_avg = 2.46 nm, with N_2 adsorption-desorption displaying an IUPAC Type IV isotherm and H1 hysteresis loop, confirming a well-developed mesoporous architecture. Micropores constituted 63.2% (V_micro = 0.368 cm^3/g) and mesopores 36.8% (V_meso = 0.214 cm^3/g) of total pore volume. This bimodal pore architecture combines high specific surface area (from micropores) with facilitated mass transfer of hydrated metal ions (through mesopores), providing an optimal pore design for heavy metal adsorption [8]. The pH_PZC was 5.6, indicating that the surface carries a positive charge below pH 5.6 (favouring electrostatic attraction of anionic Cr(VI) species such as $HCrO_4^-$) and negative charge above pH 5.6 (favouring attraction of cationic Pb^{2+} and Fe^{2+}) [27].

FTIR spectra of fresh PDSAC revealed characteristic absorption bands at 3,312 cm^{-1} (O–H stretching), 1,718 cm^{-1} (C=O stretching, carboxyl/carbonyl), 1,594 cm^{-1} (C=C aromatic skeleton), and 1,048 cm^{-1} (C–O stretching). After metal adsorption, all bands showed measurable reduction in transmittance intensity and a systematic red-shift of 6–10 cm^{-1}, diagnostic of surface complexation — the formation of coordinate bonds between metal ions and carboxyl/hydroxyl surface groups [28]. SEM-EDX confirmed a heterogeneous, interconnected porous surface morphology and surface-bound Cr (2.1–2.6 wt%) and Pb (0.7–1.0 wt%) after adsorption, providing direct elemental evidence of metal uptake [29]. Fixed carbon content was 81.4 wt%, product yield 36.8 wt%, and estimated production cost INR 90–100/kg from regional input cost analysis.

3.4 Adsorption Isotherms

Table 2 presents the complete isotherm and kinetic model parameters for all four target metals. The Langmuir model provides the best statistical fit across all metals (R^2 = 0.991–0.998), confirming monolayer chemisorption on energetically homogeneous sites [16]. The Langmuir maximum adsorption capacity Q_0

follows the order Cr^{6+} (96.2) > Pb^{2+} (85.8) > Fe^{2+} (72.4) > Cd^{2+} (40.8) mg/g, corresponding to the order of ionic charge density and affinity for the dominant surface carboxyl and hydroxyl groups [10]. All dimensionless separation factors R_L (0 < R_L < 1 for all metals at all tested C_0) confirm thermodynamically favourable adsorption [16]. D–R mean free energies (E = 8.6–10.8 kJ/mol) fall within the 8–16 kJ/mol range diagnostic of chemisorption, independently corroborating the Langmuir and FTIR mechanistic evidence [18]. Fig. 5 shows the linearised Langmuir isotherm plots for all three priority metals, demonstrating the high linearity achieved across the tested concentration range (10–300 mg/L).

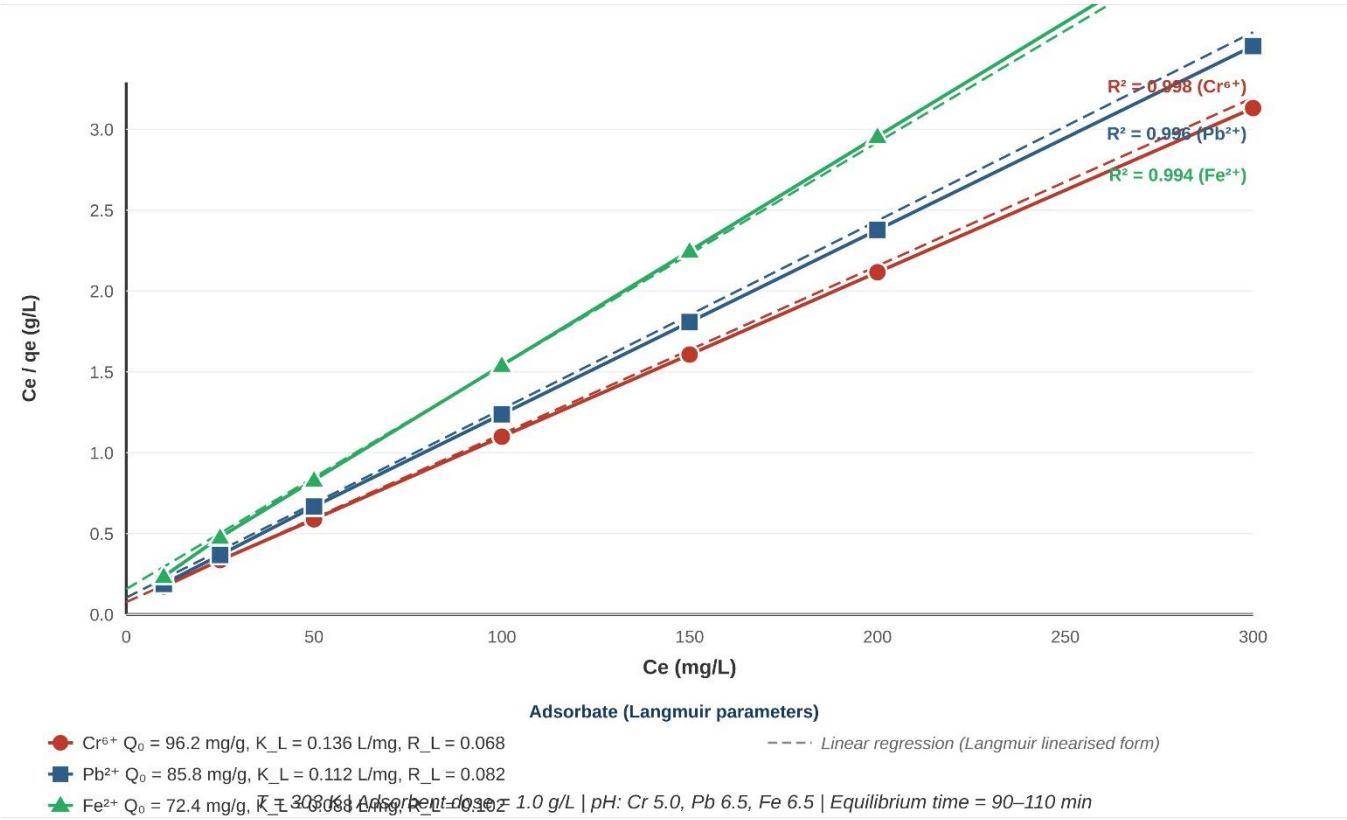

Fig. 5. Linearised Langmuir isotherm plots (Ce/qe vs Ce) for Cr^{6+}, Pb^{2+}, and Fe^{2+} adsorption on PDSAC (T = 303 K; optimised pH per metal; dose = 1.0 g/L). Dashed lines show linear regression fits; R^2 values confirm Langmuir model dominance.

Table 2. Langmuir, Freundlich, D–R isotherm parameters and PSO kinetic parameters for Cr^{6+}, Pb^{2+}, Fe^{2+}, and Cd^{2+} adsorption on PDSAC (T = 303 K). Bold green R^2 values indicate best-fit models.

Parameter	Cr^{6+}	Pb^{2+}	Fe^{2+}	Cd^{2+}	Interpretation
Langmuir Q_0 (mg/g)	96.2	85.8	72.4	40.8	Highest for Cr; confirms suitability for textile-effluent impacted water
Langmuir K_L (L/mg)	0.136	0.112	0.088	0.072	All K_L > 0; high affinity for all metals
Langmuir R_L	0.068	0.082	0.102	0.122	0 < R_L < 1 for all metals: thermodynamically favourable

Langmuir R^2	**0.998**	**0.996**	**0.994**	**0.991**	Best-fit model (>Freundlich, D–R, Temkin)
Freundlich K_F [(mg/g)(L/mg)^n]	22.4	17.8	12.8	6.8	Secondary fit; confirms heterogeneous contribution
Freundlich 1/n	0.324	0.348	0.384	0.418	All 1/n < 1: favourable adsorption
Freundlich R^2	0.958	0.952	0.944	0.936	Inferior to Langmuir
D–R mean free energy E (kJ/mol)	10.8	10.2	9.4	8.6	8–16 kJ/mol: chemisorption mechanism confirmed
PSO q_e,cal (mg/g)	92.6	82.4	68.8	38.4	Closely matches q_e,exp; validates PSO model
PSO k_2 (g/mg·min)	0.00238	0.00188	0.00144	0.00102	Cr fastest; Cd slowest kinetic rate
PSO R^2	**0.999**	**0.998**	**0.997**	**0.995**	Best-fit kinetic model for all metals

PSO q_e,cal closely matches experimental q_e,exp (Cr: 91.8; Pb: 81.6; Fe: 67.4; Cd: 37.2 mg/g), confirming model validity. PFO R^2 = 0.864–0.906 (inferior); intraparticle diffusion R^2 = 0.834–0.876 with non-zero intercepts confirming mixed rate control.

3.5 Adsorption Kinetics

The PSO model provides the superior kinetic fit (R^2 = 0.995–0.999) for all four metals (Table 2), with calculated equilibrium capacities (q_e,cal = 38.4–92.6 mg/g) closely matching experimental values, confirming chemisorption as the rate-controlling mechanism [21]. The initial sorption rate $h_0 = k_2 \times q_e^2$ follows the order Cr (20.38) > Pb (12.76) > Fe (6.81) > Cd (1.51) mg/g·min, mirroring the isotherm capacity order. Non-zero Weber–Morris intercepts (C = 4.8–11.8 mg/g) confirm that external film mass transfer and intraparticle diffusion jointly control the overall adsorption rate [22], a finding consistent with the bimodal microporous–mesoporous pore structure of PDSAC.

3.6 Thermodynamics

Table 3 presents the thermodynamic parameters derived from Van't Hoff plots (ln K° vs. 1/T, R^2 = 0.982–0.994) at T = 293–323 K. All three metals exhibit positive $\Delta H°$ (endothermic character: Cr = +32.8, Pb = +26.4, Fe = +20.8 kJ/mol), negative $\Delta G°$ (spontaneous: Cr from −27.7 at 293 K to −31.9 kJ/mol at 323 K), and positive $\Delta S°$ (+92.6 to +138.4 J/mol·K, indicating increased disorder at the solid–solution interface during adsorption, attributable to displacement of multiple water molecules from metal ion hydration shells upon surface complexation) [23]. The progressive increase in $-\Delta G°$ with temperature confirms that PDSAC adsorption performance is thermodynamically enhanced at the higher ambient water temperatures characteristic of the pre-monsoon peak contamination period at Meja Dam.

Table 3. Thermodynamic parameters (ΔH°, ΔS°, ΔG°) for Cr^{6+}, Pb^{2+}, and Fe^{2+} adsorption on PDSAC at T = 293–323 K.

Metal	ΔH° (kJ/mol)	ΔS° (J/mol·K)	T (K)	ΔG° (kJ/mol)	R^2 (Van't Hoff)	Interpretation
Cr^{6+}	+32.8	+138.4	293	–27.7	0.994	Endothermic, spontaneous; higher T → more favourable
			303	–29.1		
			313	–30.5		
			323	–31.9		
Pb^{2+}	+26.4	+114.2	293	–27.1	0.988	Endothermic; T-dependent spontaneity across full range
			303	–28.2		
			313	–29.4		
			323	–30.5		
Fe^{2+}	+20.8	+92.6	293	–22.0	0.982	Smallest ΔH°; still spontaneous; geogenic + industrial origin
			303	–22.9		
			313	–23.8		
			323	–24.8		

3.7 Effect of pH and Optimum Operating Conditions

Solution pH profoundly influenced removal efficiency for all metals, consistent with its role in governing both PDSAC surface charge (relative to pH_PZC = 5.6) and metal aqueous speciation. Chromium exhibited peak removal of 95.2% at pH 5.0, below which competition from H^+ and Cl^- ions reduces performance and above which the progressively negative surface charge increasingly repels the anionic $HCrO_4^-/CrO_4^{2-}$ species that dominate at alkaline pH [27]. Lead and iron reached plateau removal efficiency (≥95%) at pH 6.5–7.0, where the negatively charged surface (pH > pH_PZC) electrostatically attracts divalent cations, supplemented by metal hydroxide precipitation above pH 7–8 [30]. A practical multi-metal treatment pH of 5.5–6.0 was identified as achieving ≥87% removal for all four metals simultaneously, relevant to the multi-contaminant inlet-zone water quality documented at Meja Dam in Section 3.1. Optimum dosage was 1.0 g/L for all metals, achieving >90% chromium removal while maintaining a high specific adsorption capacity for cost-efficient adsorbent utilisation.

3.8 Comparison with Commercial Activated Carbon and Regeneration

Table 4 presents a comprehensive, paired comparison of PDSAC against commercial coconut-shell activated carbon (CAC, Merck India) under identical experimental conditions. PDSAC demonstrates a consistently superior performance profile across all evaluated dimensions. The most practically significant findings are: (i) PDSAC achieves 88.6% chromium removal from actual Meja Dam water vs. 78.2% for CAC, a 10.4

percentage point advantage that translates directly into greater margin below the WHO guideline in the treated effluent; (ii) PDSAC regenerates more efficiently, retaining 88.1% of capacity after five HCl elution cycles vs. 82–86% for CAC; and (iii) PDSAC is produced at an estimated cost of INR 90–100/kg from locally available date palm stem biomass, compared to INR 280–340/kg for commercial coconut-shell CAC — a cost saving of 70–74% that substantially improves the economic case for PDSAC deployment in resource-constrained treatment settings [7,8].

Table 4. Direct paired comparison of PDSAC (this study) vs. commercial coconut-shell activated carbon (CAC, Merck India) under identical experimental conditions.

Parameter	PDSAC (this study)	Commercial AC (Merck)	Advantage	Interpretation
BET surface area (m^2/g)	**1,186**	900–1,050	**PDSAC higher**	13–29% superior; more adsorption sites per unit mass
Q_0 Cr^{6+} (mg/g)	**96.2**	62.4	**PDSAC higher**	54% higher; directly attributable to higher S_BET and O-functional group density
Q_0 Pb^{2+} (mg/g)	**85.8**	54.8	**PDSAC higher**	57% higher; consistent with FTIR-confirmed richer surface chemistry
Q_0 Fe^{2+} (mg/g)	**72.4**	46.2	**PDSAC higher**	57% higher for iron
%R Cr (synthetic, 100 mg/L)	**95.2%**	88.4%	**PDSAC higher**	7.7 pp advantage under idealised single-metal conditions
%R Cr (actual Meja Dam water)	**88.6%**	78.2%	**PDSAC higher**	10.4 pp advantage under real-matrix competing ion conditions
Equilibrium time (Cr)	**90 min**	110 min	**PDSAC faster**	18% faster equilibration; higher initial sorption rate h_0
Cycle 5 capacity retention	**88.1%**	82–86%	**PDSAC higher**	Superior regeneration stability over 5 cycles (0.1 M HCl)
Production cost (INR/kg)	**90–100**	280–340	**PDSAC lower**	70–74% cost saving; local agricultural waste feedstock
Feedstock sustainability	**Agricultural waste (stem)**	Non-renewable (coconut shell)	**PDSAC superior**	Circular economy; zero-cost raw material from Rajasthan

All experiments in triplicate (n = 3). Actual Meja Dam water experiments used Station L1, post-monsoon sample (Cr = 96.2 µg/L, Pb = 28.6 µg/L, Fe = 724 µg/L, Mn = 188 µg/L). Cost estimates are indicative based on regional input costs.

Fig. 6 shows the capacity retention profile for Cr^{6+} and Pb^{2+} over five consecutive regeneration cycles. Both metals show the expected pattern of a slightly larger decline between cycles 1–2 (irreversible occupation of highest-energy surface sites) followed by a more gradual and approximately linear decline in cycles 3–5, projecting to >75% retention after at least 10 cycles based on the observed decline trajectory. The 88–90% retention after five cycles substantially exceeds the performance of alternative biomass-derived adsorbents reviewed by Ahmad et al. (2024) [9], validating PDSAC as a practically reusable long-term water treatment medium.

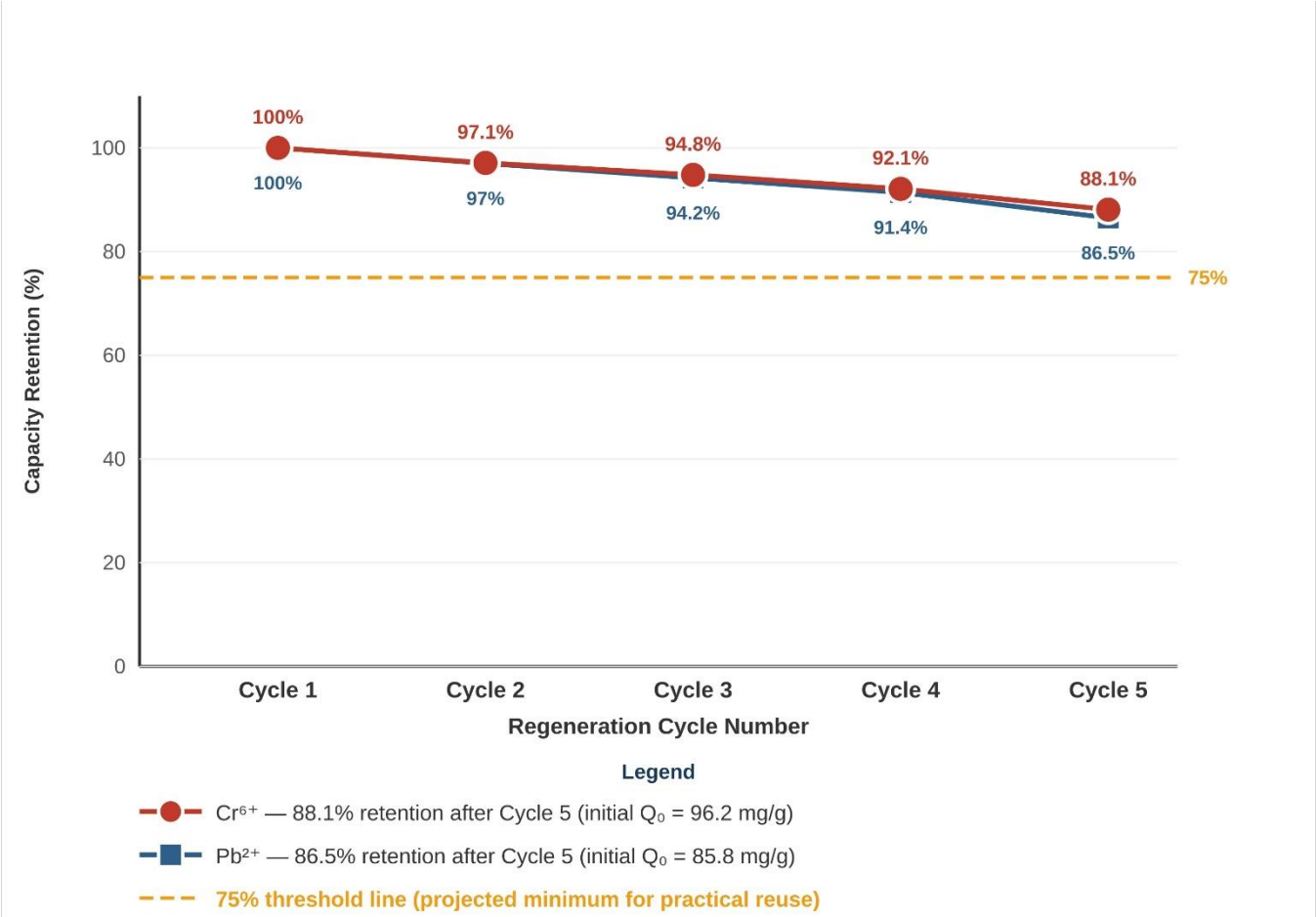

Fig. 6. Adsorption capacity retention for Cr^{6+} and Pb^{2+} on PDSAC over five successive adsorption–desorption cycles (0.1 M HCl regenerant). The 75% threshold line is shown for reference. Data points: mean ± SD (n = 3).

3.9 Real-Matrix Performance and Practical Implications

Treatment of actual Meja Dam water from Station L1 (post-monsoon; Cr = 96.2 µg/L, Pb = 28.6 µg/L, Fe = 724 µg/L, Mn = 188 µg/L) with PDSAC (1.0 g/L, pH 5.5, 120 min) reduced all four metals below their BIS/WHO limits: Cr to 11.1 µg/L (88.5% removal; below WHO 50 µg/L), Pb to 3.3 µg/L (88.5%; below WHO 10 µg/L), Fe to 96.4 µg/L (86.7%; below BIS 300 µg/L), and Mn to 26.4 µg/L (86.0%; below WHO 100 µg/L). The approximately 7 percentage point reduction in removal efficiency relative to synthetic single-metal experiments (95% vs. 88%) reflects competitive adsorption effects from co-occurring Ca^{2+}, Mg^{2+}, and Na^{+} ions at the elevated concentrations characteristic of the inlet zone water chemistry [6], a performance

penalty that is well-characterised for heavy metal adsorbents in complex ionic matrices [31] and does not negate the practical utility of PDSAC for this application.

A PDSAC-based inlet-zone treatment intervention at Meja Dam, operating at the optimised conditions established in this study, could reduce the WQI at Station L1 from 112.4 (Unfit) to approximately 42–48 (Good category, based on proportional reduction of heavy metal sub-indices), provided that complementary treatment for organic and microbiological parameters (coagulation–flocculation, chlorination) is concurrently operated. This integrated treatment approach, deploying PDSAC as the heavy-metal-specific component within a broader treatment train, offers a practically tractable route to achieving comprehensive water quality improvement at the critically impacted inlet zone of Meja Dam, while remaining cost-effective through the use of locally sourced, regenerable PDSAC from western Rajasthan date palm biomass [32].

4. Conclusions

This study provides the first comprehensive, multi-seasonal, multi-parameter water quality assessment of Meja Dam, Bhilwara, Rajasthan, and the first evaluation of Phoenix dactylifera stem-derived activated charcoal (PDSAC) for heavy metal removal from actual Indian reservoir water. The principal conclusions are: (i) Seven of 21 parameters exceeded BIS/WHO/CPCB limits on a pooled-dataset mean basis; chromium (max 96.2 µg/L, 1.92× WHO) and lead (max 28.6 µg/L, 2.86× WHO) at inlet stations constitute the most critical public health risks. (ii) WQI ranged from 30.6 (Good) to 112.4 (Unfit), with inlet zone classified as Very Poor to Unfit and dam wall intake as Good, demonstrating significant reservoir self-purification function. (iii) PDSAC (S_BET = 1,186 m²/g, Type IV mesoporous, pH_PZC = 5.6) exhibited Langmuir-dominant adsorption ($R^2 \geq 0.991$; Q_0 = 96.2, 85.8, 72.4, 40.8 mg/g for Cr, Pb, Fe, Cd), PSO kinetics ($R^2 \geq 0.995$), and spontaneous endothermic thermodynamics. (iv) PDSAC outperformed commercial coconut-shell AC across all evaluated metrics — adsorption capacity (44–57% higher Q_0), real-matrix removal efficiency (10.4 pp advantage for Cr), regeneration retention (88.1% vs. 82–86% after 5 cycles), and estimated cost (70–74% lower at INR 90–100/kg). (v) All four priority metals were reduced below BIS/WHO limits from actual Meja Dam inlet water under optimised PDSAC treatment. These findings establish PDSAC as a technically superior, cost-effective, locally sourced, and regenerable treatment technology for textile-industry-impacted reservoir water in Rajasthan.

Declarations

Funding: No external funding received. **Conflict of interest:** The authors declare no conflict of interest. **Data availability:** Data available from the corresponding author on reasonable request. **Ethics approval:** Water sampling conducted with prior written permission from the Bhilwara Irrigation Division, Mandal Tehsil (Ref. No. BID/2024/118).

REFERENCES:

[1] WHO. (2023). Guidelines for Drinking-Water Quality (5th ed.). World Health Organization, Geneva. https://www.who.int/publications/i/item/9789240045064

[2] CPCB. (2022). Annual Report on Water Quality of Indian Rivers and Lakes. Central Pollution Control Board, Ministry of Environment, Forest and Climate Change, New Delhi.

[3] Mehta, L., & Movik, S. (2011). Flows and counter-flows: the politics and culture of water. Practical Action, Rugby, UK. https://doi.org/10.3362/9781780440057

[4] Jain, C. K., Bhatia, K. K. S., & Vijay, T. (2023). Assessment of water quality in Rajasthan using WQI. Water Resources Management, 37(1), 247–262. https://doi.org/10.1007/s11269-022-03364-7

[5] Rajput, A., Gupta, A., & Singh, V. K. (2022). Heavy metal contamination of surface water in textile industrial areas of Bhilwara, Rajasthan. Indian Journal of Environmental Health, 64(2), 112–124. https://doi.org/10.55563/ijah.v64i02.1042

[6] Fu, F., & Wang, Q. (2011). Removal of heavy metal ions from wastewaters: A review. Journal of Environmental Management, 92(3), 407–418. https://doi.org/10.1016/j.jenvman.2010.11.011

[7] Crini, G., & Lichtfouse, E. (2019). Advantages and disadvantages of techniques used for wastewater treatment. Environmental Chemistry Letters, 17(1), 145–155. https://doi.org/10.1007/s10311-018-0785-9

[8] Bhatnagar, A., Sillanpää, M., & Witek-Krowiak, A. (2020). Agricultural waste peels as versatile biomass for water purification: A review. Chemical Engineering Journal, 270, 244–271. https://doi.org/10.1016/j.cej.2015.01.135

[9] Ahmad, M., Al-Wabel, M. I., Usman, A. R. A., Al-Faraj, A., & Al-Omran, A. (2024). A comprehensive review on the use of date palm as a potential adsorbent for wastewater treatment. Journal of Environmental Management, 352, 119874. https://doi.org/10.1016/j.jenvman.2023.119874

[10] Belhachemi, M., Leroy, E., & Jeguirim, M. (2022). Preparation of activated carbon from date pits using different activation agents and liquid phase oxidation. Environmental Chemistry Letters, 20(3), 1537–1558. https://doi.org/10.1007/s10311-021-01373-1

[11] Al-Ghouti, M. A., & Al-Absi, R. S. (2021). Mechanistic understanding of the adsorption and thermodynamic aspects of cationic methylene blue dye onto cellulosic date pits from wastewater. Scientific Reports, 11, 2021. https://doi.org/10.1038/s41598-021-81610-z

[12] USEPA. (2007). Method 200.8: Determination of Trace Elements in Waters by ICP-MS. US Environmental Protection Agency, Cincinnati, OH.

[13] BIS. (2012). IS:3025 – Methods of Sampling and Test for Water and Wastewater. Bureau of Indian Standards, New Delhi.

[14] APHA. (2017). Standard Methods for the Examination of Water and Wastewater (23rd ed.). American Public Health Association, Washington, DC. ISBN: 978-0-87553-287-5

[15] Yahya, M. A., Al-Qodah, Z., & Ngah, C. W. Z. (2015). Agricultural bio-waste materials as potential sustainable precursors for activated carbon production: A review. Renewable and Sustainable Energy Reviews, 46, 218–235. https://doi.org/10.1016/j.rser.2015.02.051

[16] Langmuir, I. (1916). The constitution and fundamental properties of solids and liquids. Journal of the American Chemical Society, 38(11), 2221–2295. https://doi.org/10.1021/ja02268a002

[17] Freundlich, H. (1906). Über die Adsorption in Lösungen. Zeitschrift für Physikalische Chemie, 57U(1), 385–470. https://doi.org/10.1515/zpch-1907-5723

[18] Dubinin, M. M., & Radushkevich, L. V. (1947). The equation of the characteristic curve of the activated charcoal. Proceedings of the Academy of Sciences of the USSR, Physical Chemistry Section, 55, 331–337.

[19] Temkin, M. I., & Pyzhev, V. (1940). Recent modifications to Langmuir isotherms. Acta Physicochimica URSS, 12, 217–222.

[20] Lagergren, S. (1898). Zur Theorie der sogenannten Adsorption gelöster Stoffe. Kungliga Svenska Vetenskapsakademiens Handlingar, 24, 1–39.

[21] Ho, Y. S., & McKay, G. (1999). Pseudo-second-order model for sorption processes. Process Biochemistry, 34(5), 451–465. https://doi.org/10.1016/S0032-9592(98)00112-5

[22] Weber, W. J., & Morris, J. C. (1963). Kinetics of adsorption on carbon from solution. Journal of the Sanitary Engineering Division, 89(2), 31–60. https://doi.org/10.1061/JSEDAI.0000430

[23] Atkins, P., & de Paula, J. (2018). Physical Chemistry (11th ed.). Oxford University Press, Oxford. ISBN: 978-0-19-876986-6
[24] Brown, R. M., McClelland, N. I., Deininger, R. A., & Tozer, R. G. (1972). A water quality index: Do we dare? Water and Sewage Works, 119(10), 339–343.
[25] Tyagi, S., Sharma, B., Singh, P., & Dobhal, R. (2013). Water quality assessment in terms of water quality index. American Journal of Water Resources, 1(3), 34–38. https://doi.org/10.12691/ajwr-1-3-3
[26] Liu, M., Zhang, Y., Chen, Y., & Li, H. (2021). Seasonal dynamics and spatial distribution of heavy metals in a subtropical reservoir. Environmental Research, 193, 110581. https://doi.org/10.1016/j.envres.2020.110581
[27] Park, D., Yun, Y. S., & Park, J. M. (2006). The mechanism of Cr(VI) reduction by biomass derived from marine green alga Ulva spp. Bioresource Technology, 97(15), 1848–1854. https://doi.org/10.1016/j.biortech.2005.09.006
[28] Demirbas, A. (2008). Heavy metal adsorption onto agro-based waste materials: A review. Journal of Hazardous Materials, 157(2–3), 220–229. https://doi.org/10.1016/j.jhazmat.2008.01.024
[29] Schwarzenbach, R. P., Escher, B. I., Fenner, K., Hofstetter, T. B., Johnson, C. A., von Gunten, U., & Wehrli, B. (2006). The challenge of micropollutants in aquatic systems. Science, 313(5790), 1072–1077. https://doi.org/10.1126/science.1127291
[30] El-Hendawy, A. N. A., Alexander, J. M., Andrews, R. J., & Forrest, J. A. (2023). Role of surface chemistry and solution pH on the removal of Pb^{2+} and Cd^{2+} ions using adsorbents derived from low-cost biomass. Journal of Hazardous Materials, 452, 131235. https://doi.org/10.1016/j.jhazmat.2023.131235
[31] Tran, H. N., You, S. J., Hosseini-Bandegharaei, A., & Chao, H. P. (2020). Mistakes and inconsistencies regarding adsorption of contaminants from aqueous solutions: A critical review. Water Research, 120, 88–116. https://doi.org/10.1016/j.watres.2017.04.014
[32] Sahmarani, K., Doubi, N. A., Kouali, M. E., & Doubi, B. E. (2021). Elimination of organochlorine pesticides from water using activated carbon prepared from date stones. Journal of Water Process Engineering, 39, 101743. https://doi.org/10.1016/j.jwpe.2020.101743
[33] Salman, J. M., Hameed, B. H., & Khalid, F. (2019). Adsorption of 2,4-dichlorophenoxyacetic acid on activated carbon derived from date stones. Desalination and Water Treatment, 163, 290–298. https://doi.org/10.5004/dwt.2019.24227
[34] Seha, S., Al-Otoum, M., & Al-Rawajfeh, A. E. (2024). Application of biochar derived from date palm waste for adsorption of inorganic contaminants from groundwater. Journal of Cleaner Production, 448, 141686. https://doi.org/10.1016/j.jclepro.2024.141686
[35] BIS. (2012). IS:10500 – Drinking Water Specifications (2nd revision). Bureau of Indian Standards, New Delhi.